

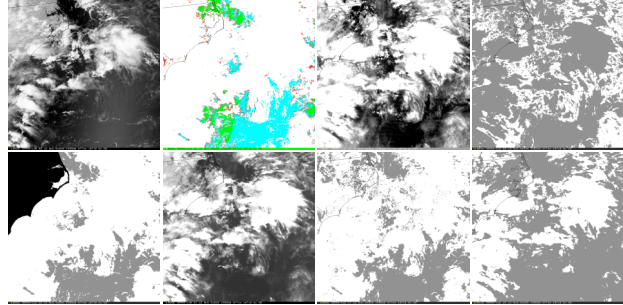
Validation and Consistency of the MODIS Cloud Mask

Richard A. Frey^a, Steven A. Ackerman^a, Kathleen I. Strabala^a, Hong Zhang^a, Andrew Heidinger^b and Michael Pavlonis^a

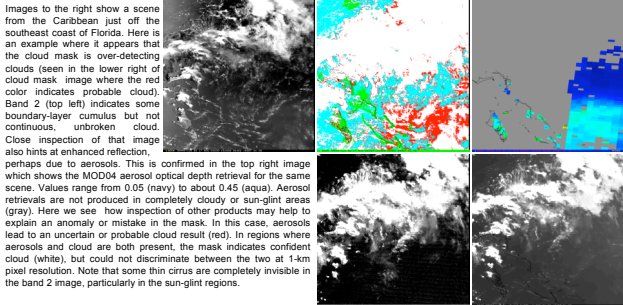
^aCooperative Institute for Meteorological Satellite Studies, Space Science and Engineering Center, University of Wisconsin-Madison
^bOffice of Research and Applications, NOAA / NESDIS, Madison, WI, USA

Validation of cloud detection algorithms is difficult. The determination of cloud amounts from the surface by purely human faculties is extremely subjective, so much more the interpretation of results from space where sensor footprint size, wavelength, even eventual use of the data influences quality assessments. There being no absolute "ground truth" data to test against, we resort to various comparisons and consistency checks. Shown below are two examples of **image analysis**, where cloud detection results are compared to imagery of the input data itself. We believe this is the most effective "first cut" at validation; cloud mask data must at least overlay obvious clouds in multi-spectral imagery. Most MODIS 5-minute data granules encompass a wide range of cloud, atmosphere, and surface characteristics over which to exercise the MOD35 algorithm, while also being a manageable amount of data to view.

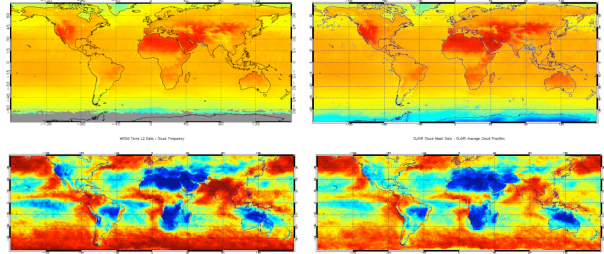
A key cloud detection quality metric is **consistency of products between instruments**. Shown below are comparisons of cloud amounts and clear-sky products from MODIS and AVHRR using the CLAVR (Clouds from AVHRR) algorithm. Also compared are cloud frequencies from MODIS and two very different measurements, the space-borne Geoscience Laser Altimeter System (GLAS) and the ground-based Micropulse Lidar/Millimeter Wavelength Cloud Radar (MPL/MIMCR).



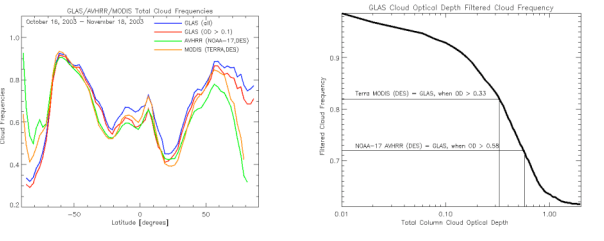
Above images show example of cloud mask validation using image analysis. Left to right and top to bottom: band 2 (0.86 μ m) reflectance, cloud mask final result, band 26 (1.38 μ m) reflectance, thin cirrus flag, SST cloud test, band 31 (11 μ m) BT, 11-12 μ m cloud test, and 1.38 μ m cloud test. In the final mask result, green indicates confident clear, cyan is probably clear, red is uncertain, white denotes confident cloud. The large proportion of probably clear pixels is due to the very being largely within a sun-glint area. The mask appears to identify almost all clouds in the various images with the exception of a few very thin cirrus seen in the band 26 image.



Images to the right show a scene from the Caribbean just off the southeast coast of Florida. Here is an example where it appears that the cloud mask is over-detecting clouds (seen in the lower right of cloud mask image where the red color indicates probable cloud). Band 2 (top left) indicates some boundary-layer cumulus but not continuous, unbroken cloud. Close inspection of that image also hints at enhanced reflection, perhaps due to aerosols. This is confirmed in the top right image which shows the MOD04 aerosol optical depth retrieval for the same scene. Values range from 0.05 (navy) to about 0.45 (aquamarine). Aerosol retrievals are not produced in completely cloudy or sun-glint areas (gray). Here we see how inspection of other products may help to explain an anomaly or mistake in the mask. In this case, aerosols lead to an uncertain or probable cloud result (red). In regions where aerosols and cloud are both present, the mask indicates confident cloud (white), but could not discriminate between the two at 1-km pixel resolution. Note that some thin cirrus are completely invisible in the band 2 image, particularly in the sun-glint regions.

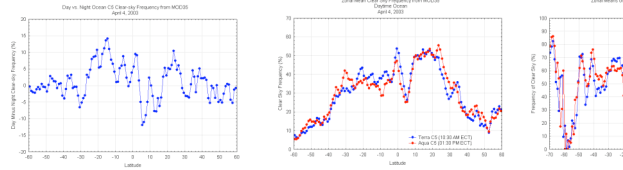


Monthly mean clear-sky 11 μ m BTs derived using the MODIS cloud mask (top left) and CLAVR (top right) for the month of July, 2002 are shown above. The maps are remarkably similar with only a few regions in Asia and sea-ice boundaries showing significant differences. Shown immediately above are global cloud frequencies for July 2004 from the MODIS cloud mask (left) and from AVHRR using CLAVR. Note that the main climatological features are being captured by both algorithms. The main difference between the two seems to be that the MODIS algorithm finds more clouds in predominantly cloudy regions (N. Pacific, southern ocean) and less clouds in mainly clear areas (subtropical Pacific and Atlantic, western US). The clear-sky AVHRR data is from GAC ascending node NOAA-16, the cloud frequency data is from NOAA-17 GAC descending node. Shown below left are zonal cloud frequencies from several instruments, including the GLAS. The plot below at right shows GLAS cloud amounts calculated using only observations with an optical depth greater than or equal to the value given on the x-axis. Lines show where Terra MODIS and NOAA-17 AVHRR CLAVR had cloud amounts equal to GLAS.

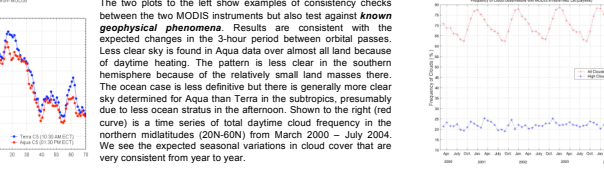


Radar/Lidar	MODIS Cloud	MODIS Uncertain	MODIS Probably Clear	MODIS Clear
Clear	19	6	85	65
Low Cloud	82	4	3	175
Middle Cloud	44	3	13	30
High Cloud	14	1	6	24
	159	10	108	71

The MODIS cloud mask algorithm and the ARM CART MPL/MIMCR agreed on the existence of clear or probably clear 86% of the time (86+5/175) and 92% of the time that a cloud was present (see table at left). An uncertain result occurred in less than 3% of the total comparisons.

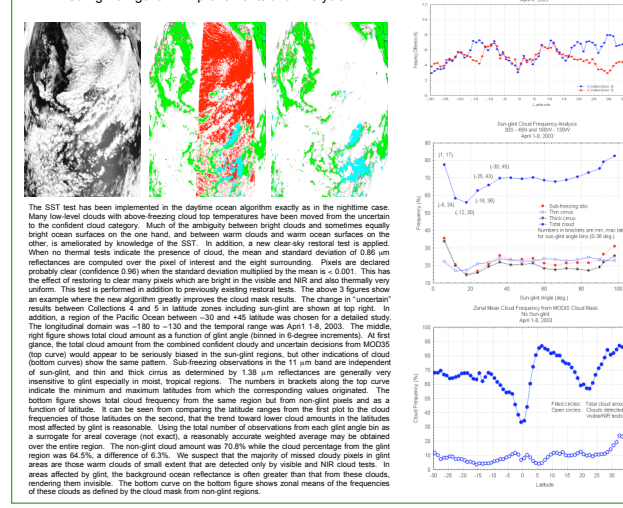


Shown below and below right are examples of **consistency checks** used to ascertain the quality of the MOD35 product. When changes were made to the sun-glint and night ocean algorithms for Collection 5, ways were needed to determine overall cloud detection quality in these scenes but also the consistency between sun-glint and no sun-glint and between day and night results. Image analysis could show dramatic improvements in some granules (below), but did not address the consistency issues over multiple days. See also the plot at above left that shows day minus night ocean clear-sky frequencies for a day of Terra data.



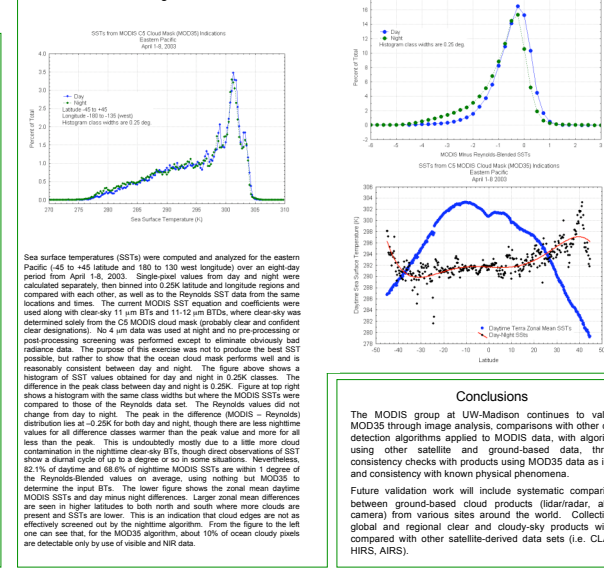
The two plots to the left show examples of consistency checks between the two MODIS instruments but also test against known **geophysical phenomena**. Results are consistent with the expected changes in the 3-hour period between orbital passes. Less clear sky is found in Aqua data over almost all land because of daytime heating. The pattern is less clear in the southern hemisphere because of the relatively small land masses there. The ocean case is less definitive but there is generally more clear sky determined by Aqua than Terra in the subtropics, presumably due to less ocean stratus in the afternoon. Shown to the right (red curve) is a time series of total daytime cloud frequency in the northern midlatitudes (20N-60N) from March 2000 - July 2004. We see the expected seasonal variations in cloud cover that are very consistent from year to year.

Sun-glint Algorithm Improvements and Analysis



The SST test has been implemented in the daytime ocean algorithm exactly as in the nighttime case. Many low-level clouds with above-heating cloud top temperatures have been moved from the uncertain to the confident cloud category. Much of the ambiguity between bright clouds and sometimes equally bright ocean surfaces on the one hand, and between warm clouds and warm ocean surfaces on the other, is ameliorated by knowledge of the SST. In addition, a new clear-sky restoral test is applied. When no thermal tests indicate the presence of cloud, the mean and standard deviation of 0.86 μ m reflectance are computed over the pixel of interest and the eight surrounding. Pixels are declared probably clear (confidence 0.98) when the standard deviation multiplied by the mean is < 0.001 . This has the effect of restoring to clear many pixels which are bright in the visible and NIR and also thermally very uniform. This test is performed in addition to previously existing restoral tests. The above 3 figures show an example where the new algorithm greatly improves the cloud mask results. The change in "uncertain" results between Collections 4 and 5 in latitude zones including sun-glint are shown at top right. In addition, a region of the Pacific Ocean between -30 and $+45$ latitude was chosen for a detailed study. The longitudinal domain was -180 to $+180$ and the temporal range was April 1-8, 2003. The middle-right figure shows total cloud amount as a function of glint angle (binned in 6-degree increments). At first glance, the total cloud amount from the combined confident cloudy and uncertain decisions from MOD35 (top curve) would appear to be seriously biased in the sun-glint regions, but other indications of cloud (bottom curves) show the test works. Sub-restoring observations in the 11 μ m band are independent of sun-glint, and thin and thick cirrus as determined by 1.38 μ m reflectance are generally very insensitive to glint especially in most, tropical regions. The numbers in brackets along the top curve indicate the minimum and maximum latitudes from which the corresponding values originated. The bottom figure shows total cloud frequency from the same region but from non-glint pixels and as a function of latitude. It can be seen from comparing the latitude ranges from the first plot to the cloud frequencies of those latitudes on the second, that the trend toward lower cloud amounts in the latitudes most affected by glint is reasonable. Using the total number of observations from each glint angle bin as a surrogate for areal coverage (not exact), a reasonably accurate weighted average may be obtained over the entire region. The non-glint cloud amount was 70.8% while the cloud percentage from the glint region was 64.5%, a difference of 6.3%. We suspect that the majority of missed cloudy pixels in glint areas are those warm clouds of small extent that are detected only by visible and NIR cloud tests. In areas affected by glint, the background ocean reflectance is often greater than that from these clouds, rendering them invisible. The bottom curve on the bottom figure shows zonal means of the frequencies of these clouds as defined by the cloud mask from non-glint regions.

Sea Surface Temperature Analysis Using MOD35



Sea surface temperatures (SSTs) were computed and analyzed for the eastern Pacific (45 to 48 latitude and 180 to 130 west longitude) over an eight-day period from April 1-8, 2003. Single-pixel values from day and night were calculated separately, then binned into 0.25K latitude and longitude regions and compared with each other, as well as to the Reynolds SST data from the same locations and times. The current MODIS SST equation and coefficients were used along with clear-sky 11 μ m BTs and 11-12 μ m BTs, where clear-sky was determined solely from the CS MODIS cloud mask (probably clear and confident clear designations). No 4 km data was used at night and no pre-processing or post-processing screening was performed except to eliminate obviously bad radiance data. The purpose of this exercise was not to produce the best SST possible, but rather to show that the ocean cloud mask performs well and is reasonably consistent between day and night. The figure above shows a histogram of SST values obtained for day and night in 5 K classes. The difference in the peak class between day and night is 0.25K. Figure at top right shows a histogram with the same class widths but where the MODIS SSTs were compared to those of the Reynolds data set. The Reynolds values did not change from day to night. The peak in the difference (MODIS - Reynolds) distribution lies at $-0.25K$ for both day and night, though there are less nighttime values for all difference classes warmer than the peak value and more for all less than the peak. This is undoubtedly mostly due to a little more cloud contamination in the nighttime clear-sky BTs, though direct observations of SST show a diurnal cycle of up to a degree or so in some situations. Nevertheless, 82.1% of daytime and 88.6% of nighttime MODIS SSTs are within 1 degree of the Reynolds-blended values on average, using nothing but MOD35 to determine the input BTs. The lower figure shows the zonal mean daytime MODIS SSTs and day minus night differences. Larger zonal mean differences are in higher latitude to both north and south where thin clouds are present and SSTs are lower. This is an indication that cloud edges are not as effectively screened out by the nighttime algorithm. From the figure to the left one can see that, for the MOD35 algorithm, about 10% of ocean cloudy pixels are detectable only by use of visible and NIR data.

Conclusions

The MODIS group at UW-Madison continues to validate MOD35 through image analysis, comparisons with other cloud detection algorithms applied to MODIS data, with algorithms using other satellite and ground-based data, through consistency checks with products using MOD35 data as input, and consistency with known physical phenomena. Future validation work will include systematic comparisons between ground-based cloud products (lidar/radar, all-sky camera) from various sites around the world. Collection 5 global and regional clear and cloudy-sky products will be compared with other satellite-derived data sets (i.e. CLAVR, HIRS, AIRS).